

Analysis of the Stationary and Transient Behavior of a Photovoltaic Solar Array: Modeling and Simulation

Carlos D. Rodríguez Gallegos
Energy Conversion and Storage Institute,
Ulm University
Helmholtzstraße 18
89081 Ulm, Germany

Manuel S. Alvarez Alvarado
Department of Electrical and Computer
Engineering, New Jersey Institute of Technology
University Heights Newark
07102 New Jersey, United States of America

ABSTRACT

The behavior of a photovoltaic solar array is investigated by performing a simulation in Simulink (MATLAB). The modeling of the system is based on the one diode model (in which the solar cell's equivalent circuit is composed by a current source, diode, series and parallel resistance). The simulation results show how the series and parallel connection of the solar cells have a direct impact under the maximum voltage and current that the array can generate, respectively. The linear dependence of the array's current with respect to the solar irradiance is also exposed. Not only its stationary performance but also its transient behavior is discussed by adding a capacitor on the model to represent the influence of the charge separation that occurs at the depletion region.

General Terms

Pattern Recognition, Performance, Algorithms.

Keywords

Solar Array, Mathematical Model, Simulation, Stationary and Transient State.

1. INTRODUCTION

In our society, the amount of people is increasing in time, as a result, more industries, houses and transportation systems are required and by this, a higher demand of electrical energy is needed [1]. Most of this demand is covered by means of non-renewable energy sources. Nevertheless, these sources are limited and in the future, a scenario with no available sources of energy can be reached. Here comes the need to focus in the research of different renewable energy systems [2].

Photovoltaics appears as a very interesting field to generate energy with a potential to have a high development in the future [3]. The production of solar cells is increasing in time [4] due to their advantages:

- Direct conversion of the energy from the light into electricity.
- No moving components (opposite to wind generators or hydro plants), no losses or damage due to friction.
- High application range as they can be employed to power portable devices, houses, towns, among others.

In this paper, the physical principle of the photovoltaic effect takes place in order to obtain the mathematical model of the solar cell and the solar array. This model is then simulated in Simulink and the obtained results are discussed.

2. ELECTRICAL MODEL OF A SOLAR CELL

A solar cell is an element in which the photovoltaic effect [5] is present. This effect consists in the direct generation of electricity from light. To represent it with equations, it is necessary to take into account its physical properties. The solar cell, as in most of the cases, is a Silicon semiconductor material [6] which is divided into two regions, one doped by a n-material (like Phosphorous) to provide free electrons and the other region doped by a p-material (like Boron) to provide free holes. A semiconductor with a p-n junction has the behavior of a diode "D" [7].

When the photons impact the solar cell, if they have enough energy, they will release and generate an electron-hole pair that contributes to the photovoltaic current " I_{ph} " (current produced inside the solar cell due to the photovoltaic effect). This means that if the number of photons (with enough energy) is increased, the value of the photovoltaic current will increase with the same proportion (assuming an ideal case). Hence, a direct relation between the solar irradiance and the photovoltaic current can be considered.

There are also resistivity losses within the solar cell. For instance, the resistance present at the metallic contacts (fingers and busbars), at the intersection between the semiconductor and the metallic contacts, at the semiconductor, among others. All of these losses are represented as the series resistance " R_s ".

The shunt resistance (also called parallel resistance) " R_p " takes into account the losses due to short circuits within the cell, a typical outcome from manufacturing defects.

At the junction between the p-n junction of the solar cell, an effective charge is produced by cations (positive ions at the n side) and anions (negative ions at the p side), this small region is known as the "depletion region". It can then be understood that at the junction, there are positive charges in one side and negative charges in the other. For simplicity, these charges can be considered to be separated by an average distance which is the thickness of the depletion region. As a result of the split charges, the effect of a capacitor, with capacitance " C ", is present; this can be described by the parallel plate capacitor.

All of these parameters are reflected in Fig. 1.

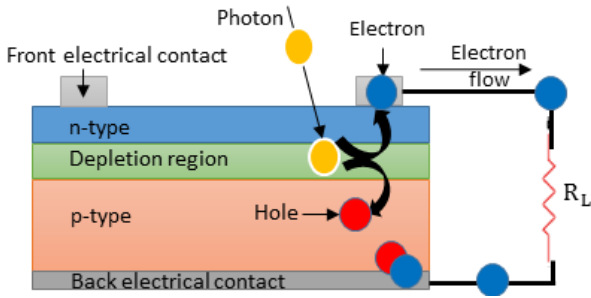


Fig 1: Schematic of the photovoltaic effect

The electrical model of a solar cell is represented in Fig. 2.

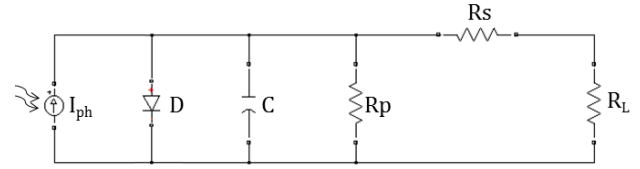


Fig 2: Electrical circuit of a solar cell

3. ELECTRICAL AND MATHEMATICAL MODEL OF A SOLAR ARRAY

A solar array consists on a number of solar cells connected in series and/or parallel among them. From the electrical model of the solar cell, it can easily be concluded that the equivalent model of a solar array is as the one shown in Fig. 3 [8].

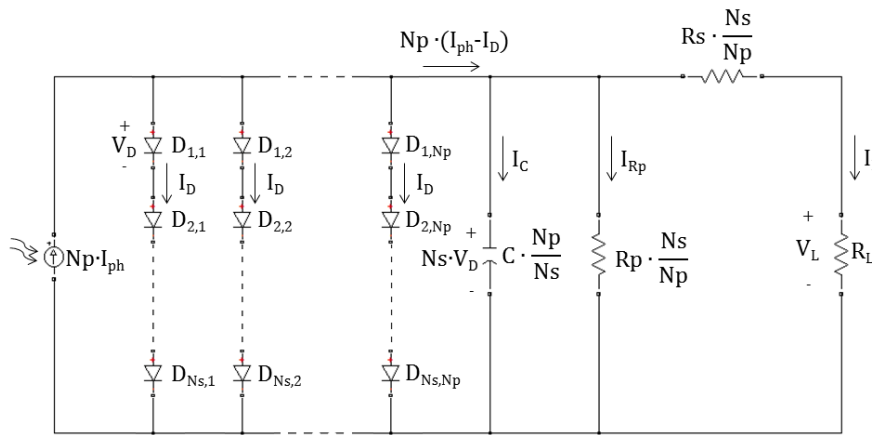


Fig 3: Electrical circuit of a solar array

In which:

Ns: Number of solar cells connected in series.

Np: Number of solar cells connected in parallel.

V_D: Diode voltage.

I_D: Current through a diode.

R_L: Load resistance (external resistance).

V_L: Load voltage (output voltage).

I_L: Load current (output current).

The procedure to obtain a mathematical expression for V_L takes place in the following paragraphs. It is based on the electrical circuit from the previous figure.

It can be noticed that the total photovoltaic current (N_p · I_{ph}) is divided among the diodes (N_p · I_D), capacitor (I_C), shunt resistance (I_{Rp}) and the load (I_L). By employing the Kirchhoff Nodal rule, the following equation can be obtained:

$$N_p \cdot I_{ph} = N_p \cdot I_D + I_C + I_{Rp} + I_L \quad (1)$$

The relation between the current and voltage of a diode is expressed by the Shockley equation [9]. An extra parameter known as the ideality factor “n” is considered, its value reveals the degree of influence of the recombination mechanisms:

$$I_D = I_0 \cdot \left(e^{\frac{e^- \cdot V_D}{n \cdot K_B \cdot T}} - 1 \right) \quad (2)$$

In which:

I₀: Dark saturation current (constant of a solar cell that depends on parameters such as the free carrier’s diffusivity and the doping level).

e⁻: Electron charge (1.602176565×10⁻¹⁹ C).

K_B: Boltzmann constant (8.6173324×10⁻⁵ eV/K).

T: Temperature of the solar cell or array.

The current of the capacitor I_C is related with its voltage V_C in the following way [10]:

$$I_c = \left(C \cdot \frac{N_p}{N_s} \right) \cdot \frac{d(V_C)}{dt} = \left(C \cdot \frac{N_p}{N_s} \right) \cdot \frac{d(N_s \cdot V_D)}{dt} \quad (3)$$

In which the term $C \cdot \frac{N_p}{N_s}$ represents the total capacitance of the capacitor from Fig. 3.

By using Ohm’s law, the following relations are found:

$$I_{Rp} = \frac{N_s \cdot V_D}{\frac{N_s}{N_p} \cdot R_p} \quad (4)$$

$$I_L = \frac{V_L}{R_L} \quad (5)$$

By replacing Eq. (2), (3), (4) and (5) in (1), Eq. (6) is generated.

$$N_p \cdot I_{ph} = N_p \cdot I_o \cdot \left(e^{\frac{e^{-V_D}}{n \cdot k_B \cdot T}} - 1 \right) + C \cdot N_p \cdot \frac{d(V_D)}{dt} + \frac{N_p \cdot V_D}{R_p} + \frac{V_L}{R_L} \quad (6)$$

Eq. (6) appears only in terms of V_L and the constants of the system, except by V_D that is not a constant. An expression for the diode voltage in terms of the constants and the load voltage is then necessary.

The voltage of the diodes can be related with the ones of the series and load resistance using the Kirchhoff Voltage rule:

$$N_s \cdot V_D = \frac{N_s \cdot R_s}{N_p} \cdot I_L + V_L = \frac{N_s \cdot R_s}{N_p} \cdot \frac{V_L}{R_L} + V_L \quad (7)$$

Solving Eq. (7) for V_D :

$$V_D = \frac{V_L}{N_s} \cdot \left(1 + \frac{N_s \cdot R_s}{N_p \cdot R_L} \right) \quad (8)$$

Finally, by replacing Eq. (8) in (6) and solving for V_L :

$$V_L = \frac{N_p \cdot I_{ph} - N_p \cdot I_o \cdot \left(e^{\frac{e^{-\frac{V_L}{N_s} \cdot \left(1 + \frac{N_s \cdot R_s}{N_p \cdot R_L} \right)}}{k_B \cdot T}} - 1 \right) - \frac{C \cdot N_p}{N_s} \cdot \left(1 + \frac{N_s \cdot R_s}{N_p \cdot R_L} \right) \cdot \frac{d(V_L)}{dt}}{\frac{N_p}{R_p \cdot N_s} \cdot \left(1 + \frac{N_s \cdot R_s}{N_p \cdot R_L} \right) + \frac{1}{R_L}} \quad (9)$$

The load voltage appears at both sides of Eq. (9). To obtain its value, iterative methods are employed in Simulink.

The constants of the solar array that are considered in this simulation are within the typical range of values for crystalline silicon solar cells, such as:

At a solar irradiance of 1000 W/m^2 , I_{ph} is assumed to be equal to “ $30 \text{ mA/cm}^2 \cdot \text{cell area}$ ”. I_{ph} depends on the area of the solar cell because, the bigger its area, the more photons it can absorb. It is also proportional to the irradiance as explained in section 2.

Solar cells with an area of 239 cm^2 , $R_p=1000 \Omega$, $R_s=0.01 \Omega$, $I_o=1 \cdot 10^{-10} \text{ A}$ and $T=298\text{K}$ (ambient temperature) are considered.

The values for N_s , N_p and C depend on the considerations for each simulation.

The model created in Simulink is presented in Fig. 4.

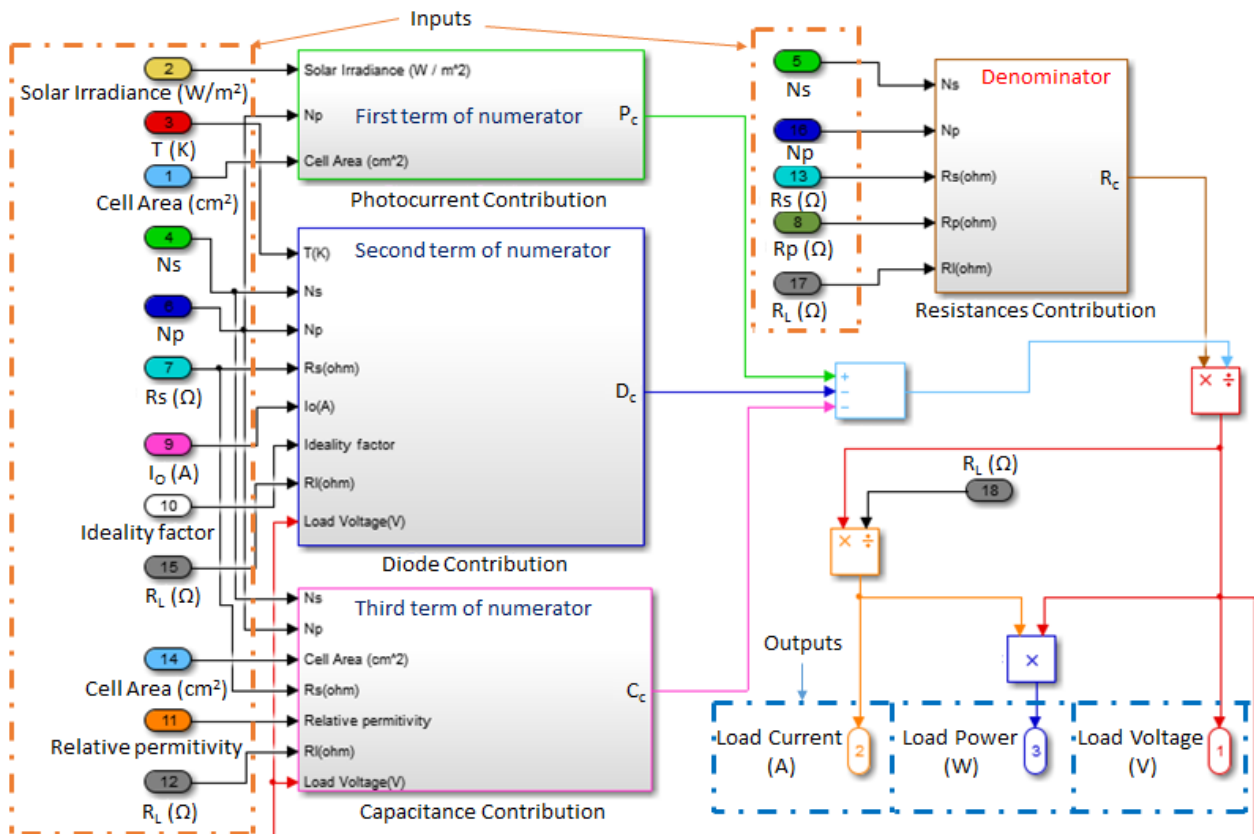


Fig 4. Solar array model implemented in Simulink

Fig. 4 is the representation of Eq. (9), it can be observed that there are four principal blocks. The first one named “Photocurrent Contribution” (P_c) corresponds to the first term

of the numerator of Eq. (9) and it provides the relation between I_{ph} and the solar irradiance (as explained in the last section), as shown in Fig. 5.

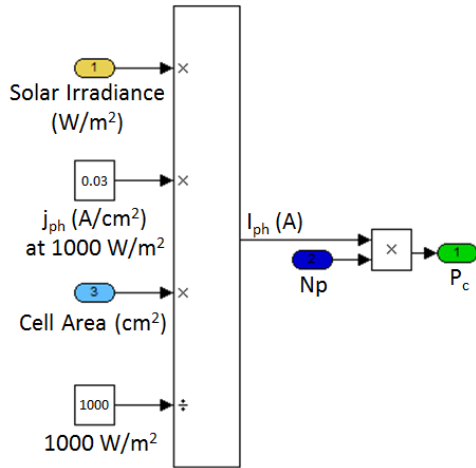


Fig 5: Relation between I_{ph} and the solar irradiance

The second block, named “Diode Contribution” (D_c), corresponds to the second term of the numerator of Eq. (9).

$$D_c = N_p \cdot I_o \cdot \left(\exp \left(\frac{e^- \cdot \frac{V_L}{N_S} \cdot \left(1 + \frac{N_S \cdot R_S}{N_P \cdot R_L} \right)}{K_B \cdot T} \right) - 1 \right) \quad (10)$$

The third block is named “Capacitance Contribution” (C_c), it corresponds to the third term of the numerator of Eq. (9).

$$C_c = \frac{C \cdot N_p}{N_S} \cdot \left(1 + \frac{N_S \cdot R_S}{N_P \cdot R_L} \right) \cdot \frac{d(V_L)}{dt} \quad (11)$$

The fourth block, named “Resistances Contribution” (R_c), corresponds to the denominator of Eq. (9).

$$R_c = \frac{N_p}{R_P \cdot N_S} \cdot \left(1 + \frac{N_S \cdot R_S}{N_P \cdot R_L} \right) + \frac{1}{R_L} \quad (12)$$

Thus, from these four blocks, the value for V_L can be obtained. At the end of the simulation, this voltage is divided by R_L in order to obtain I_L and by multiplying V_L into I_L, the load power P_L is calculated. These are the three outputs of interest.

4. SYSTEM SIMULATION

The results of the simulations given in the following pages can be separated in two categories. The first one analyzes the stable state behavior of the solar array (no effect of the capacitor) and the second one the transient behavior including its capacitive effect to observe how much this one affects its response.

The parameters in the following simulations correspond to the ones indicated in section 3.

4.1 Solar Cell Behavior: Stationary State

These simulations study the performance of a single solar cell and provide a good understanding on how it works under different conditions.

4.1.1 IV Curve of a Solar Cell

Fig. 6 shows the performance of a single solar cell by plotting the relation of the load current and voltage. It can be appreciated how it is formed from the contribution of both, the diode IV curve and the photovoltaic current [11].

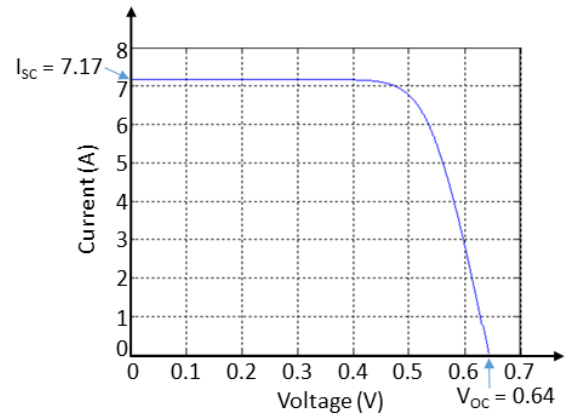


Fig 6: IV curve of a single solar cell

From the previous figure, two important parameters can be measured. The first one is the open circuit voltage (V_{OC}), which is the voltage obtained from the solar cell when the external resistance is set to infinite, the obtained value is 0.64 V. The second one is the short circuit current (I_{SC}), which is the current generated at the output of the cell when the load is set to zero, 7.17 A is the simulation result. This value seems to be the same as the photovoltaic current (I_{ph} = 30 mA/cm² · 239 cm²). However, from the electrical circuit in Fig.2, it can be understood that I_{ph} is higher than I_{SC}, being R_s an influential factor that determines how big this difference is (the bigger R_s, the smaller I_{SC}). At the present simulation, the same value is obtained for both currents because the quantities are represented up to two decimals and the set value for R_s is small enough.

4.1.2 Efficiency and Power Curve of a Solar Cell

The power produced by the cell, which is the one of the external load, is obtained by multiplying the load current into the load voltage as shown in Fig. 7, in which the “x” axis corresponds to the load voltage.

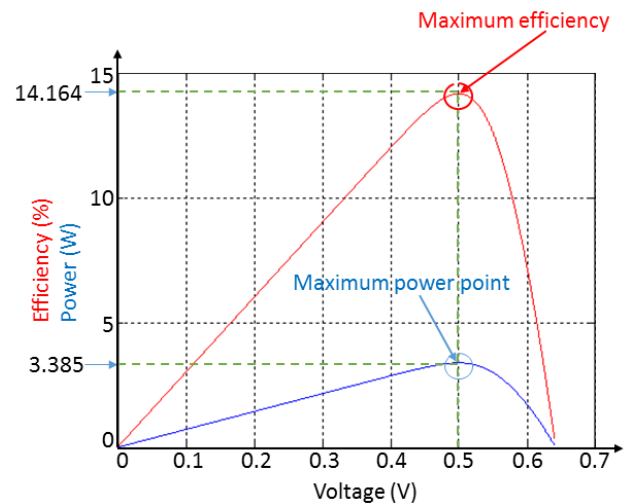


Fig 7: Efficiency and power curve of a single solar cell

The efficiency is defined as the relation between the output power (shown in the previous graph) with respect to the input power (the power coming from the sunlight into the solar cell). It is calculated with the following equation:

$$\eta = \frac{\text{Out Power}}{\text{Input Power}} \cdot 100\% = \frac{V_L \cdot I_L}{1000 \frac{\text{W}}{\text{m}^2} \cdot 0.0239 \text{ m}^2} \cdot 100\% \quad (13)$$

The behavior of the solar cell's efficiency vs the external voltage is also presented in Fig. 7.

At both graphs, when there is no voltage or current produced at the output of the cell, the power and efficiency are zero; this means that there is a point in which these values reach a maximum. In this simulation, the maximum power and efficiency are obtained at a load voltage of 0.50 V. From this graph, the maximum power point (MPP) is 3.39 W and the maximum efficiency is 14.16%. If this simulation would have assumed a better metallization quality, antireflection coating, passivation layers, among others [12], a higher efficiency would have been obtained. To the best of the authors' knowledge, the current highest efficiency for a Silicon-based solar cell is 25.6% [13] and the maximum theoretical value is about 30% [14].

An advantage of the photovoltaic system in comparison with other renewable energy systems (like the wind generators or hydro plants) is that the maximum power and efficiency are both at the same operational point. In normal conditions, the solar arrays are set to work at the MPP.

Another important parameter that can be calculated from this graph is the Fill Factor (FF), defined as:

$$FF = \frac{MPP}{V_{oc} \cdot I_{sc}} \cdot 100\% \quad (14)$$

By replacing the values from the previous equation:

$$FF = \frac{3.39W}{0.64V \cdot 7.17A} \cdot 100\% = 73.88\% \quad (15)$$

The highest the FF value, the best, as it represents the cell quality. It is equal to the proportion of the internal rectangle formed by the voltage and current at the maximum power point (orange color) with respect to the external rectangle formed by the V_{oc} and I_{sc} (green color), as shown in Fig. 8.

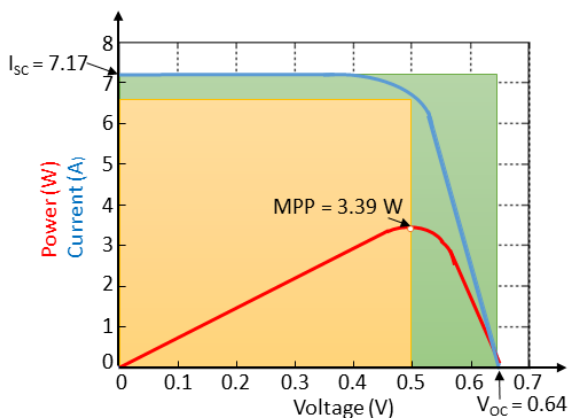


Fig 8: Fill factor calculation by rectangles proportion

4.1.3 Solar Irradiance Influence on Solar Cells

As explained in section 2, the value of I_{ph} is proportional to the amount of solar irradiance that the cell receives. In the following graph, the IV curve of a solar cell is obtained for different values of solar irradiance (600, 800, 1000 and 1200 W/m^2).

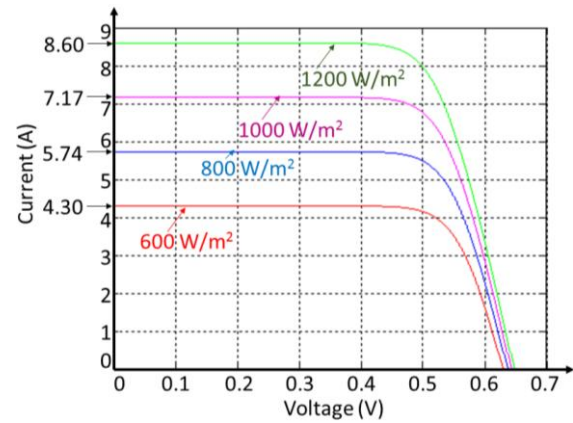


Fig 9: IV curve under different solar irradiances

From the previous graph, it is found that the proportion by which the power of the solar irradiance is increased, is the same as the increment of the I_{sc} . As explained in section i, the value of I_{sc} is similar to the one of I_{ph} .

An interesting fact is that the V_{oc} has a small increase with respect to the increase of the power of solar irradiance and it does not take place in a linear way. This is because the relation between V_{oc} and I_{ph} is logarithmic [15].

4.2 Solar Array Behavior: Stationary State

In section 4.1, the power of a single solar cell was analyzed. However, if the load of interest (TV, refrigerator, among others) requires a higher power, it is then necessary to employ more solar cells, which can be connected in series or parallel to increase the maximum voltage and current, respectively.

All the simulated solar cells have the same parameters and are identical among them (as defined in section 3).

4.2.1 IV Curve of Solar Cells in Series Connection

In most of the cases, solar panels are formed by solar cells that are connected in series, as the voltage produced by a single cell is too low for several applications. The number of interconnected solar cells depends on the amount of power desired to be generated.

Fig. 10 shows the IV behavior of the solar cells connected in series. To distinguish the different curves, a nomenclature is employed in which, the first term corresponds to the number of solar cells connected in series followed by an S (series) and finally SC (solar cell). For example, two solar cells connected in series are represented by 2S SC.

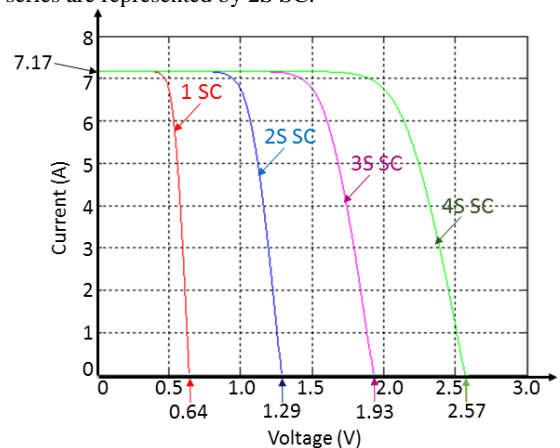


Fig 10: IV curve of series connected solar cells

It can be noticed that, regardless of the number of cells connected in series, the short circuit current remains constant with the same value as the one measured for the case of a single solar cell (Fig. 6). The number of cells in series is proportional to the increase of the open circuit voltage. For example, three solar cells in series provide a V_{OC} which is three times higher than the one of a single cell.

Hence, it can be understood that a series connection of solar cells increases the total power by increasing the external voltage.

4.2.2 IV Curve of Solar Cells in Parallel Connection

Connecting cells in parallel generates an increase in the current of the total system, as shown in Fig. 11. For the employed nomenclature, the first term corresponds to the number of solar cells connected in parallel followed by a P (parallel) and finally SC (solar cell). For example, three solar cells connected in parallel are represented by 3P SC.

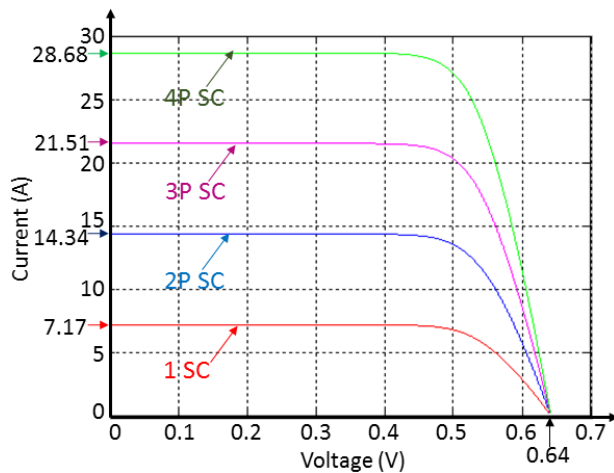


Fig 11: IV curve of parallel connected solar cells

The V_{OC} has a constant value, equal to the one of a single solar cell (Fig. 6), regardless of the amount of cells in parallel.

The number of cells in parallel connection indicates how much the I_{SC} of the whole system is increased. For example, three solar cells in parallel provide a short circuit current three times higher than the one of one solar cell.

4.2.3 IV Curve of Solar Cells in Series and Parallel Connection

This simulation represents the behavior of both, parallel and series connections.

The nomenclature is as follows:

- 1 SC: For a single solar cell.
- 2S2P SC: System composed of two solar cells connected in series and one extra cell in parallel to each of the previous ones, having four cells in total.
- 3S3P SC: System composed of three solar cells connected in series and two extra cells in parallel to each of the previous ones, having nine cells in total.
- 4S4P SC: System composed of four solar cells connected in series and three extra cells in parallel to each of the previous ones, having 16 cells in total; and so on.

As expected, the results from Fig. 12 show the series and parallel contribution in which the system of 2S2P SC, 3S3P SC, 4S4P SC has two, three and four times, respectively, the V_{OC} and I_{SC} of a single solar cell.

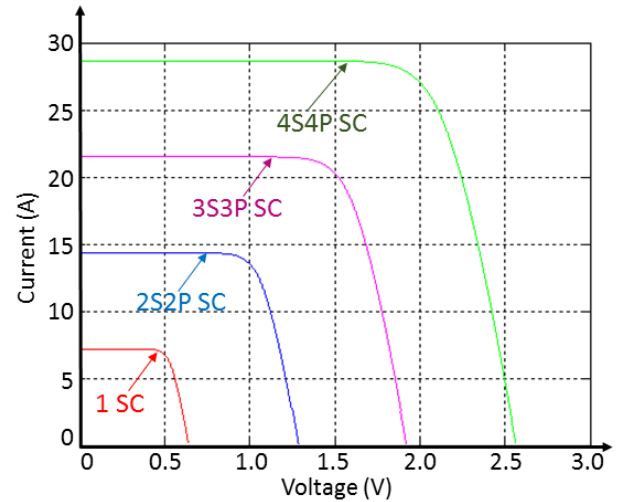


Fig 12: IV curve of series-parallel connected solar cells

4.3 Transient Behavior

In this section, the analysis of the capacitive effect of a solar cell, represented in Fig. 2, takes place.

An abrupt change in the power of the solar irradiance (from 700 W/m^2 up to 1000 W/m^2 in less than 0.0001 seconds) takes place in order to observe how strong is the capacitive behavior of the system (a high capacitive means that regardless of the increase in the power of the solar irradiance, a high opposition to the change in voltage will be present).

The capacitor component has been analyzed in section 2. It is modelled as a parallel plate capacitor in which Eq. (16) is applied [10].

$$C = \frac{\epsilon_r \cdot \epsilon_0 \cdot A}{d} \quad (16)$$

In which, " ϵ_r " represents the relative permittivity of the material (11.8 for Silicon), " ϵ_0 " is the vacuum permittivity ($8.85 \cdot 10^{-12} \text{ F/m}$), " A " is the area of the solar cell and " d " is the width of the depletion region.

Depending on the cell technology, the characteristics of the depletion region, such as its width, are modified. Two cases are analyzed: crystalline silicon and thin film solar cells.

4.3.1 Transient Behavior of a Crystalline Silicon Solar Cell

The standard silicon substrate thickness is in the range of $200 \mu\text{m} - 240 \mu\text{m}$ [16] and the width of the depletion region is considered to be $0.35 \mu\text{m}$ for this simulation (this value is obtained by assuming a built in potential of 0.75 eV, acceptor concentration in the p material of 10^{16} per cm^3 and donor concentration in the n material of 10^{16} per cm^3) [17]. From Eq. (16), a capacitance of $7.13 \mu\text{F}$ is calculated.

By employing the previous conditions, the irradiance, output voltage and output current of this solar cell are plotted in Fig.13.

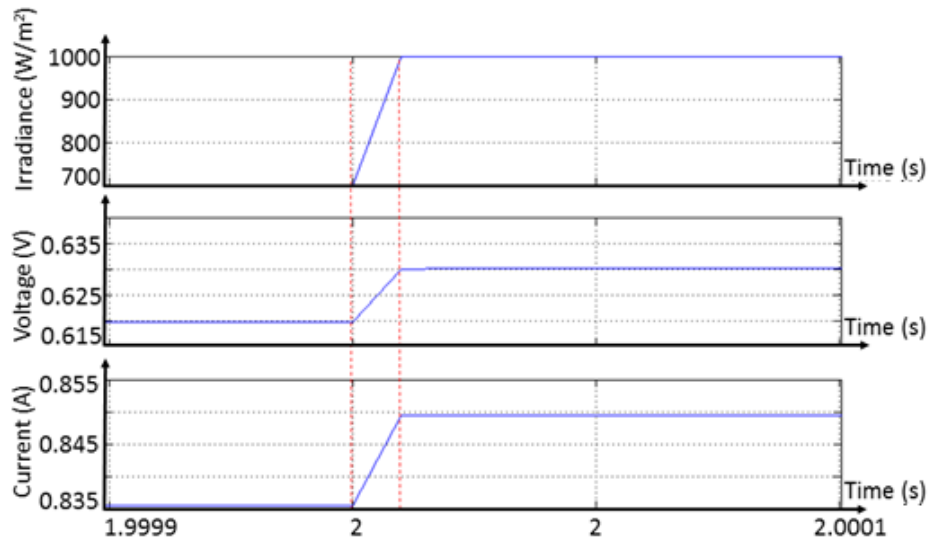


Fig 13: Crystalline Si solar cell transient behavior

From the previous figure, it can be concluded that the capacitance of this solar cell is too small as it does not seem to oppose to the change in voltage because, when the solar irradiance varies linearly, the voltage and the current also change linearly without presenting any opposition.

4.3.2 Transient Behavior of Thin Film Technologies

Thin film technologies, as its name indicates, produce thinner solar cells (from few nanometers up to tens of micrometers [18]) in comparison to the crystalline silicon ones. For this simulation, the width of the depletion region is assumed to be 10 nm. From Eq. (16), a capacitance of 249.59 μF is calculated. The simulation results are shown in Fig. 14.

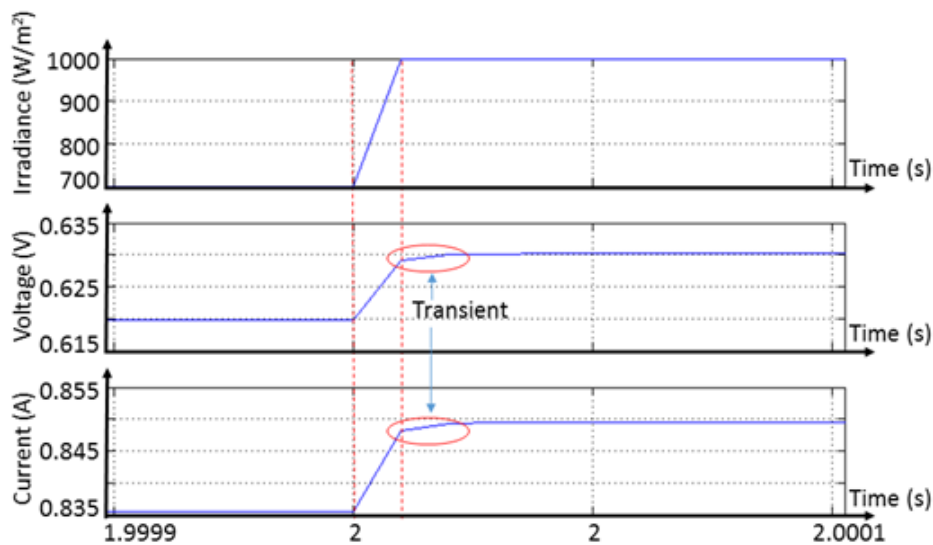


Fig 14: Thin film solar cell transient behavior

It can be noticed that just after the solar irradiance reaches the value of 1000 W/m^2 and stays constant, the output voltage and current are still changing on time (they require more time to stabilize as compared with the crystalline silicon solar cells). For this technology, the value of the capacitance is high enough to appreciate a change within the simulation when such a transient takes place.

5. CONCLUSIONS

The present paper analyzes in detail the behavior of solar cells and arrays at the transient and stationary state by performing a simulation based on the one diode model.

A solar array has different operational points depending on factors such as the value of the solar irradiance, temperature, external resistance, among others. For practical applications, the external resistance has to be fixed in order to always work at the maximum power point so that most of the solar energy is converted into useful electricity.

By connecting solar cells in series, a lineal increase in the open circuit voltage is obtained and a similar outcome, with respect to the short circuit current, occurs by connecting them in parallel. It was also shown how the photovoltaic current is proportional to the solar irradiance.

The capacitance of crystalline silicon solar cells seems to be too small in order to show an appreciable response to abrupt changes of the weather conditions. This is the reason why in most of the simulations, the capacitor component is disregarded. Thin film solar cells, with such a thin depletion region, have a higher transient response than crystalline silicon solar cells.

The present investigation serves as the starting point to analyze the performance of the whole photovoltaic system, which is expected to be performed in future research.

6. REFERENCES

- [1] A. Caillé, et al., “2007 Survey of Energy Resources”, World Energy Council 2007, 2007.
- [2] S. Mittal, et al., “Tapping the Untapped: Renewing the Nation”, Discussion Paper, CUTS CITEE, Jaipur, pp. 13-16, 2012.
- [3] B. P. Nelson, “The Potential of Photovoltaics”, NREL/CP-520-44105, 2008.
- [4] E. Despotou, et al., “Global Market Outlook for Photovoltaics until 2014”, The European Photovoltaic Industry Association (EPIA), Brussels, 2010.
- [5] K. Lehovec, “The Photo-Voltaic Effect”, Physical Review Letters, vol. 74(4), pp. 463-471, 1948.
- [6] C. Kittel, “Introduction to Solid State Physics”, 7th ed., John Wiley & Sons, Inc., USA, pp. 197-232, 1996.
- [7] W. D. Callister, et al., “Materials Science and Engineering an Introduction”, 7th ed., John Wiley & Sons, Inc., New York, USA, pp. 694-696, 2007.
- [8] M. Alvarez, et al., “Mathematical Model of a Separately Excited DC Motor Powered by a Solar Array Using External Starter Resistances”, Latin-American Journal of Physics Education, vol. 8(4), pp. 4305-1-6, 2014.
- [9] C. J. Chen, “Physics of Solar Energy”, 1st ed., John Wiley & Sons, Inc., New Jersey, USA, pp. 174, 2011.
- [10] A. R. Hambley, “Electrical Engineering Principles and Applications”, 5th ed., Pearson, USA, pp.125-136, 2011.
- [11] F. A. Lindholm, et al., “Application of the superposition principle to solar-cell analysis”, IEEE Transactions on Electron Devices, vol. 26(3), pp. 165-171, 1979.
- [12] D. H. Neuhaus, et al., “Industrial Silicon Wafer Solar Cells”, Advances in Optoelectronics, vol. 2007, Article ID 24521, 15 pages, 2007.
- [13] M. A. Green, et al., “Solar Cell Efficiency Tables (Version 45)”, Progress in Photovoltaics, vol. 23(1), pp. 1-9, 2015.
- [14] W. Shockley, et al., “Detailed Balance Limit of Efficiency of p-n Junction Solar Cells”, Journal of Applied Physics, vol. 32(3), pp. 510-519, 1961.
- [15] A. McEvoy, et al., “Practical Handbook of Photovoltaics Fundamentals and Applications”, 1st ed., Elsevier Ltd, United Kingdom, pp. 72-75, 2003.
- [16] T. Saga, “Advances in crystalline silicon solar cell technology for industrial mass production”, NPG Asia Materials, vol. 2(3), pp. 96-102, 2010.
- [17] M. Muhibbullah, et al., “An Equation of the Width of the Depletion Layer for a Step Heterojunction”, Transactions of the Materials Research Society of Japan, vol. 37(3), pp. 405-408, 2012.
- [18] J. Poortmans, et al., “Thin Film Solar Cells: Fabrication, Characterization and Applications”, 5th ed., John Wiley & Sons, Inc., USA, pp. xix, 2006.